Chapter 10

TiO_2: A Critical Interfacial Material for Incorporating Photosynthetic Protein Complexes and Plasmonic Nanoparticles into Biophotovoltaics

Yiqun Yang and Jun Li

Additional information is available at the end of the chapter

http://dx.doi.org/10.5772/intechopen.68744

Abstract

TiO_2, a photosensitive semiconducting material, has been widely reported as a good photoanode material in dye-sensitized solar cells and new emerging perovskite cells. Its proper electronic band structure, surface chemistry and hydrophilic nature provide a reactive surface for interfacing with different organic and inorganic photon capturing materials in photovoltaics. Here, we review its enabling role in incorporating two special materials toward biophotovoltaics, including photosynthetic protein complexes extracted from plants and plasmonic nanoparticles (e.g., gold or silver nanoparticles), which interplay to enhance the absorption and utilization of sun light. We will first give a brief introduction to the TiO_2 photoanode, including preparation, optical and electrochemical properties, and then summarize our recent research and other related literature on incorporating photosynthetic light harvest complexes and plasmonic nanoparticles onto anatase TiO_2 photoanodes as a means to tap into the charge separation, electron and energy transfer, and photovoltaic enhancements in the bio-photovoltaics.

Keywords: photoanode, dye-sensitized solar cells, photosynthetic protein complexes, charge separation, plasmonic effect, interface, Schottky barrier, energy transfer, hot electrons

1. Introduction

As a photosensitive semiconductor material with good long-term stability, nontoxicity, low cost and abundance, TiO_2 has been widely used in photocatalysis and photovoltaics [1]. However, due to the wide band gap (i.e., 3.0 eV for rutile and 3.2 eV for anatase TiO_2, respectively), pristine TiO_2 only responds to the irradiation in UV region. It is inefficient for capturing the majority

of photons lying in the visible range of the normal solar irradiation spectrum. Decorating visible-light-excitable compounds, so-called photo-sensitizers or dyes, on TiO_2 can effectively overcome this issue, which has been adopted to develop dye-sensitized solar cells (DSSCs) [2].

The operation principle of DSSCs is illustrated in **Figure 1**. Organic dyes anchored on TiO_2 surface are excited by absorbing visible light in the specific wavelength range. The charge separation occurs at the sensitizer/TiO_2 interface by injecting electrons from the excited state of the dye into the TiO_2 conduction band to generate free electrons, which are then diffused through the sintered TiO_2 nanoparticle layer and external circuit to the cathode to generate a photocurrent. Concurrently, the oxidized dye is reduced to its ground state by oxidation of the redox mediator I^- into I_3^-, with I_3^- ions then diffusing through the electrolyte to the cathode and reduced back to I^- by accepting electrons combing back from the external circuit to complete the whole regeneration process. Overall, this system converts solar energy into electricity without any net consumption of chemicals, and thus, the DSSC can continuous supply power under irradiation by sun light. In 2011, a porphyrin sensitized DSSC incorporated with $Co^{II/III}$ tris(bipyridyl) redox electrolyte achieved a record-high power conversion efficiency (PCE) of 12.3% [4]. Recently, a new emerging perovskite solar cell using solid-state mesoscopic TiO_2 photoanode sensitized with lead halide perovskite ($CH_3NH_3PbX_3$) was reported to achieve an exciting PCE of more than 15% [5], and it quickly approached to 20% by post-treatment of mesoporous TiO_2 photoanodes with lithium salts [6].

The prototype of DSSC is analogue to the photosynthesis in plants taking place at thylakoid membrane in the chloroplast composed of various photosynthetic proteins. **Figure 2** depicts the light-dependent reactions in the photosynthesis. Briefly, solar energy is absorbed by exciting the light harvesting complexes (i.e., LHCI and LHCII), a kind of proteins binding a lot of chlorophylls (Chls) as major pigments in the photosystems (PSI and PSII). The excitation

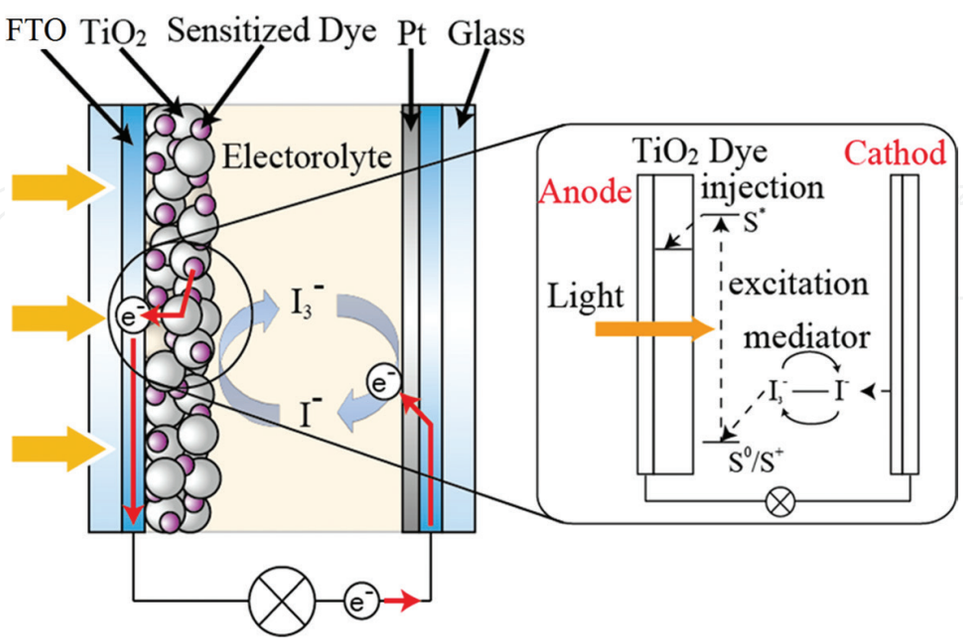

Figure 1. Structure and operating mechanism of a DSSC. Reprinted with permission of Ref. [3].

http://dx.doi.org/10.5772/intechopen.68744

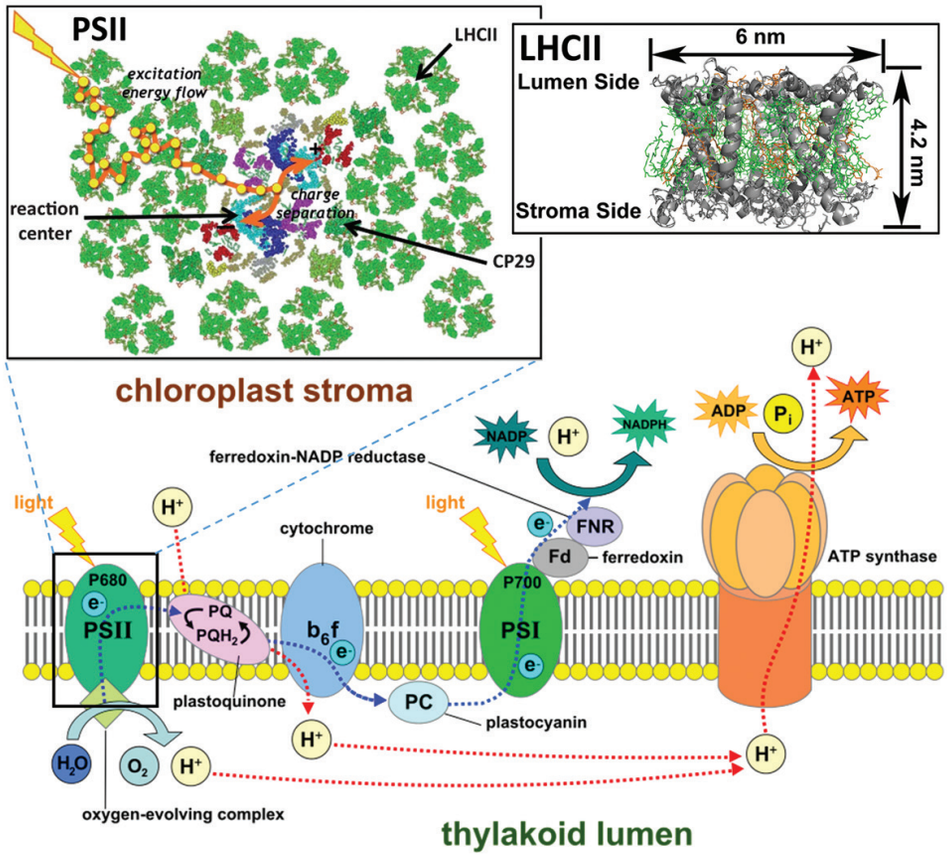

Figure 2. Photoreactions in photosynthesis at the thylakoid membrane of plant cells. Inset: the energy flow in PSII and the structure of LHCII trimer. Adapted with permission of Refs. [7, 8].

energy is resonantly transferred to the associated reaction centers (RCs) where the energy is converted into electrons by exciting a special pair of Chls, triggering a series of chemical reactions, such as water splitting in PSII, reduction of $NADP^+$ to NADPH in PSI and ATP synthesis. Inset of **Figure 2** shows components of PSII and the energy flow therein. The largest PSII supercomplex, $C_2S_2M_2$, consists of a dimeric core complex (C_2) containing RCs, 4 monomeric minor antenna complexes (CP29), 4 strongly attached LHCII trimers (S_2 and M_2), and 3–4 loosely attached LHCII trimers [9]. LHCII trimer is the most abundant Chl-protein complex in nature and the major antenna complex in PSII. The LHCII trimer consists of three monomers each of which comprises a polypeptide of about 232 amino-acid residues, 8 Chl *a* and Chl *b* molecules, 3–4 carotenoids and one phospholipid [10].

It should be noted that both photosynthesis systems and DSSCs utilize separate media for photon capture and energy transfer (executed by the excitation of LHCs and photosensitizers, respectively) and charge separation (occurs in RCs and the dye/TiO_2 interface, respectively). This mechanism has an advantage to reduce the possibility of charge recombination [11]. Owing to such similarity, various DSC architectures have been explored to directly use natural extracted pigments [12, 13] and photosynthetic LHCs [14–17] as photosensitizers to replace synthetic dyes in developing biophotovoltaic cells. Although the biophotovoltaic cells have much lower PCE than normal DSSCs, these hybrid systems serve as a unique platform

to study the crucial processes including charge separation and transport at the interface of TiO_2 photoanode with natural photosensitizers and provide insights into the limiting factors. In this chapter, we will summarize our recent research and other related literature on incorporating photosynthetic proteins and plasmonic nanoparticles (PNPs) onto anatase TiO_2 photoanodes as a means to tap into the charge separation, electron and energy transfer processes, and plasmonic enhancement in the biophotovoltaics. The following aspects will be involved: (i) configuration and surface modification of TiO_2 photoanode, (ii) energy state coupling and charge transfer between photosynthetic proteins and TiO_2, (iii) plasmonic effects on biophotovoltaics, and (iv) hot electrons across Schottky barrier at Au/TiO_2 interface.

2. Configuration and surface modification of TiO_2 photoanode

2.1. Fabrication of TiO_2 photoanode

Conventional photoanode in DSSCs is composed of a 10-μm-thick nanostructured TiO_2 film prepared from deposition and sintering of spherical TiO_2 nanoparticles (NPs) on conducting fluorine doped tin oxide (FTO) glass. This mesoporous layer has a large surface area for dye adsorption while maintaining a percolation network for electron transport. Later, a variety of TiO_2 nanorods, nanowires and networks were designed to replace the spherical NPs in photoanode [18–20]. These structures are regarded with more efficient electron transport pathway owing to the inherent well-aligned crystalline domains and the greater electron diffusion length [21, 22]. Typically, the TiO_2 nanomaterials are synthesized by sol-gel method, then dispersed with surfactants into a paste and coated on FTO glass via doctor-blade casting, spin coating or screen printing. This multi-step route is tedious and induces large variances in prepared TiO_2 layers. The electron diffusion in the layer is restrained by large boundary. Instead, direct growth of highly ordered architectures on substrates is among the most exciting developments for novel photoanodes. Vertically aligned TiO_2 nanotube arrays have been successfully produced by potentiostatic anodization of titanium metal in a fluoride containing electrolyte and exhibit larger electron diffusion length [23]. A forest-like photoanode combining efficient light trapping and high surface area for dye absorption was synthesized via fine control of pulse laser deposition, which consists of hierarchical assemblies of nanocrystalline particles of anatase TiO_2 [24]. This hierarchical architecture was demonstrated to suppress electron recombination with tri-iodide along with increase of electron lifetime and perform no hindering in mass transport using ionic liquid electrolyte. Recently, we employed a similar anatase TiO_2 nanotree array as photoanode scaffold for the LHCII sensitized biophotovoltaic cells [25]. This TiO_2 nanotree array can be simply grown on TiO_2 coated FTO glass by one-pot hydrothermal reaction without necessity of high-tech equipment [26]. The transmission electron microscopy (TEM) and scanning electron microscopy (SEM) images in **Figure 3** confirm the morphology of the TiO_2 nanotrees prepared by this method. Each nanotree is composed of 6-μm-long TiO_2 nanowire trunk covered by short and thinner branches extending sideway. The growing model is illustrated in **Figure 4**, showing a hierarchical assembly of TiO_2 nanostructure in which the number and length of branches on the TiO_2 nanowire trunk can be increased with the longer reaction time.

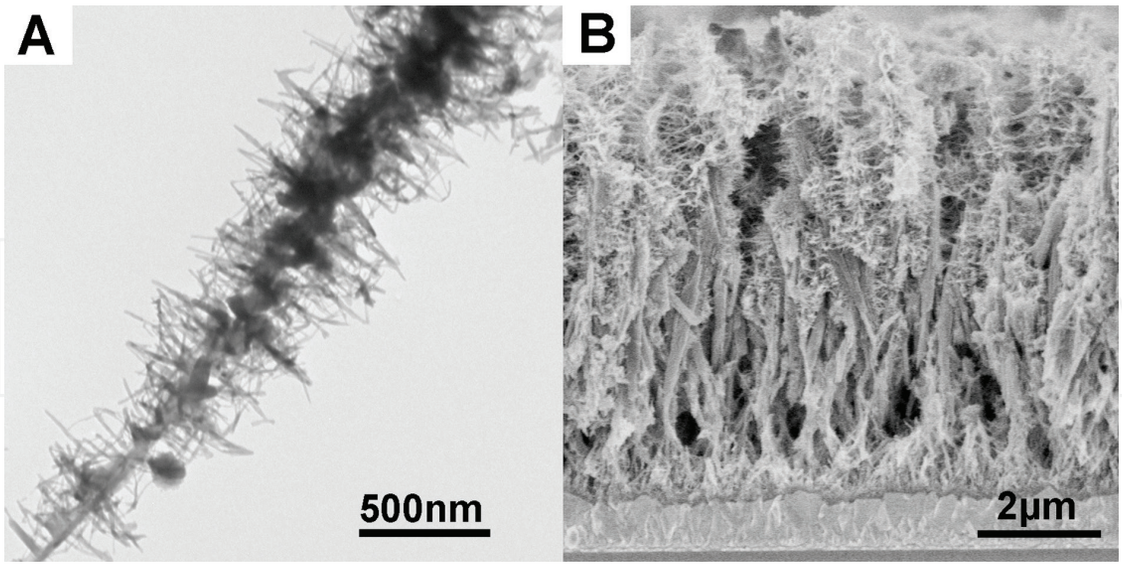

Figure 3. (A) TEM image of the TiO_2 nanotree scraped off from the FTO substrate and (B) the cross-sectional view of TiO_2 nanotree array by SEM. Reprinted with permission of Ref. [27].

In addition, post-synthesis thermal treatment can be applied to attain highly crystalline TiO_2 photoanodes. Due to higher dye loading and faster electron transport rate, the TiO_2 with pure anatase phase is more favorable than rutile phase in photoanode applications [28]. The crystallization strongly depends on annealing process. It normally yields the anatase phase if the annealing temperature is below 550°C but tends to form the thermodynamically stable rutile phase at higher temperatures [29]. The XRD (**Figure 5A**) and Raman (**Figure 5B**) characterizations confirmed that single crystalline anatase phase was attained for the TiO_2 nanotrees subjected to 500 °C calcination for 30 min.

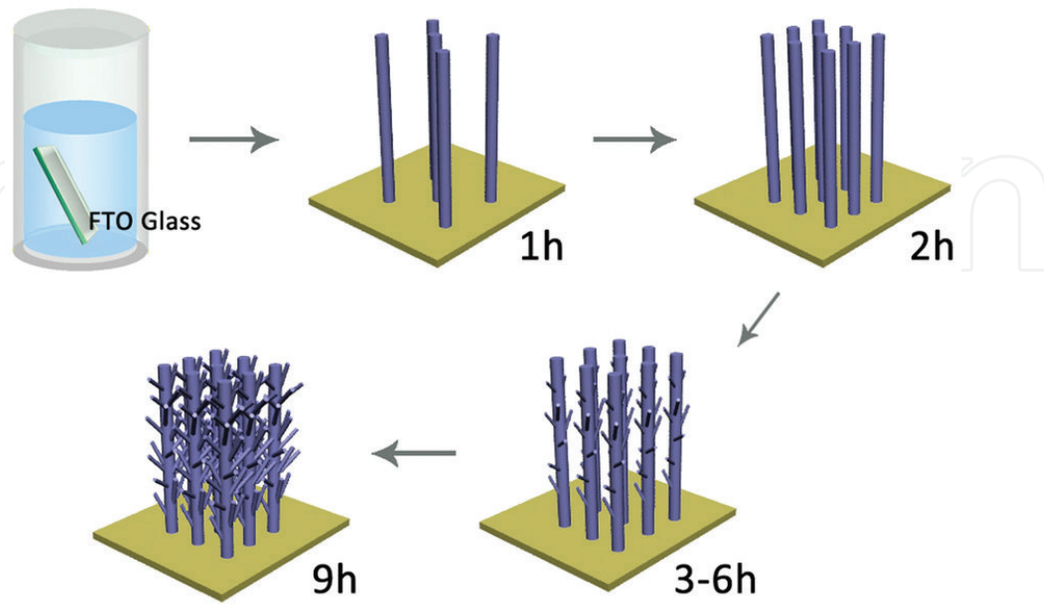

Figure 4. Schematic formation process of the hierarchical anatase TiO_2 nanotree arrays on FTO substrates. Reprinted with permission of Ref. [26].

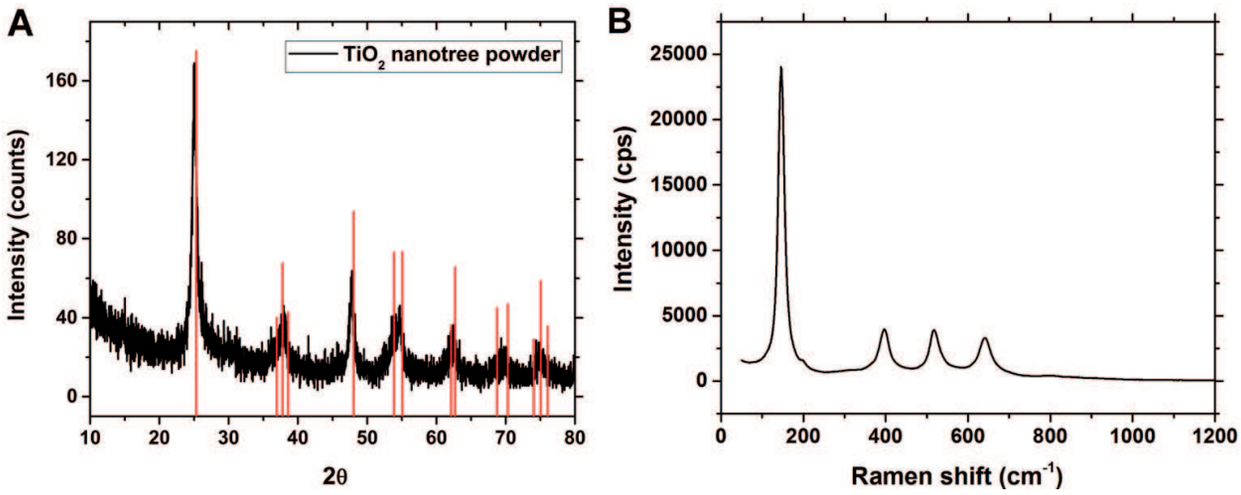

Figure 5. (A) XRD pattern and (B) Raman spectrum of the TiO_2 nanotrees after 500 °C thermal annealing. The standard XRD peak position of anatase TiO_2 (JCPDS card No 71–1166) is indicated as the vertical red lines in (A). Reprinted with permission of Ref. [26].

2.2. TiO_2 barrier layer

In the photoanode of DSSCs, besides using TiO_2 for charge separation and electron transport, a thin compact TiO_2 layer of tens to hundreds of nanometers is usually deposited between mesoporous TiO_2 nanoparticle film and transparent conductive oxide (TCO) coated glass as a barrier layer. This barrier layer was found to be critical in impairing the electron backflow at the TCO/electrolyte interface, increasing the shunt resistance, and therefore increasing the fill factor and overall cell efficiency [30, 31], as depicted in **Figure 6A**.

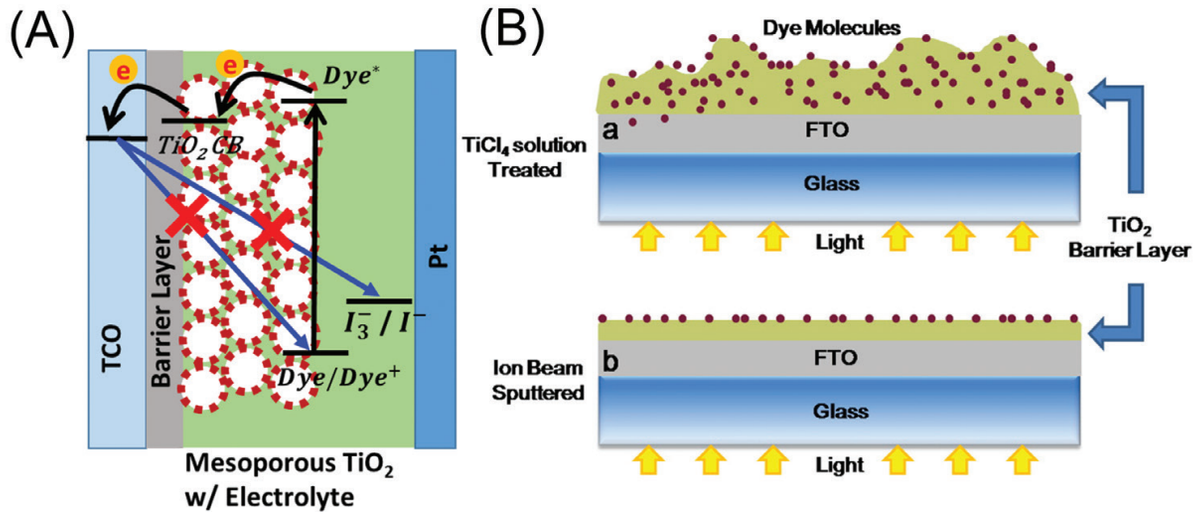

Figure 6. (A) Charge recombinations in DSSC due to the electron back flow from TCO to oxidized dye and redox electrolyte. (B) Illustration of the differences of the TiO_2 barrier layers formed by (a) $TiCl_4$ treatment and (b) Ti sputtering followed by thermal annealing. Adapted with permission of Ref. [32].

To establish a reliable planar photoanode for biophotovoltaics, we systematically studied the TiO_2 barrier layer deposited by two distinct methods and correlated the TiO_2 structure with its barrier properties [32]. **Figure 6B** schematically shows that a porous dye-penetrable TiO_2 film was attained by the $TiCl_4$ solution treatment, while a conformal compact TiO_2 film was obtained by sputtering-annealing Ti. The latter seemed to be an ideal barrier layer since dye molecules can only adsorb on the external TiO_2 surface. However, the performance of DSSCs made with the sputtering-annealing method was worse than those by $TiCl_4$ treatments due to the lower electrical conductivity since anatase structure is mixed with amorphous and rutile phases in the film. In this work, the DSSCs fabricated with photoanodes by 20 min $TiCl_4$ treatment showed the best performance, likely due to the formation of desired anatase crystallites with the optimum thickness. Such thin-film DSSC was used as a model system to test the photovoltaic effects of photosynthetic proteins that cannot easily access the interior pores of traditional mesoporous DSSCs.

2.3. Biosensitizations on surface modified TiO_2 photoanodes

One complication to fabricate biophotovoltaic devices is to integrate biophotosensitizers with artificial semiconductors in photoanode. Unlike synthetic dyes that can easily use various anchoring groups, for example, carboxylate (—COOH), phosphonate ($—H_2PO_3$) or siloxy moiety ($—O—SiR_3$), through molecular engineering to increase binding affinity to metal oxide semiconductor [33, 34], chemical modifications on natural extracted photosynthetic protein complexes would cause unfavorable structural changes that impair their intrinsic photoelectric properties. Although the photosynthetic protein complexes contain carboxylate groups in their polypeptide matrix, they are usually extracted and dispersed in aqueous buffer solution in which the strong polar water solvent and the surfactants tend to break the adsorption equilibrium causing desorption from the metal oxide surface. Addition of binding agents is desired to conjugate photosynthetic protein complexes to artificial photoanodes. Mershin et al. bioengineered PSI with a designed peptide surfactant that contains an amino acid sequence with specific high binding affinity to ZnO (**Figure 7**) [35]. In the study, the native electron acceptor subunit PsaE within PSI was substituted with the ZnO-binding peptide tag: RSNTRMTARQHRSANHKSTQRARS to promote attachment and orientation of the PSI on ZnO nanowires. Thus, the modified PSI was preferentially bound to ZnO nanowires by the electron acceptor side, minimizing the electron traveling distance between electron acceptor and electrode and maximizing the electron transfer.

Beyond introducing the specific linkers through delicate bioengineering on photosynthetic protein complexes, another simpler method to improve the protein attachment is to perform surface modifications on photoanode materials with binding molecules. Dihydroxyacetone phosphate was reported as a suitable linker between PSI and metal oxide. The indium-tin oxide (ITO) and titanium suboxide (TiO_x, x = 1, 2) substrates covered with a self-assembled monolayer of dihydroxyacetone phosphate can immobilize a densely packed PSI layer by electrostatic and hydrogen bond interactions with the polar stroma and lumen faces of PSI [36]. LHCII of PSII can also be isolated and appointed as photosensitizers in biophotovoltaic cells. However, the physisorption of LHCII on the TiO_2 photoanode was found to be very weak and unstable, as indicated by the long incubation time (96 hours) required to reach saturated adsorption [45]. It was recently reported that strong LHCII attachment can be obtained

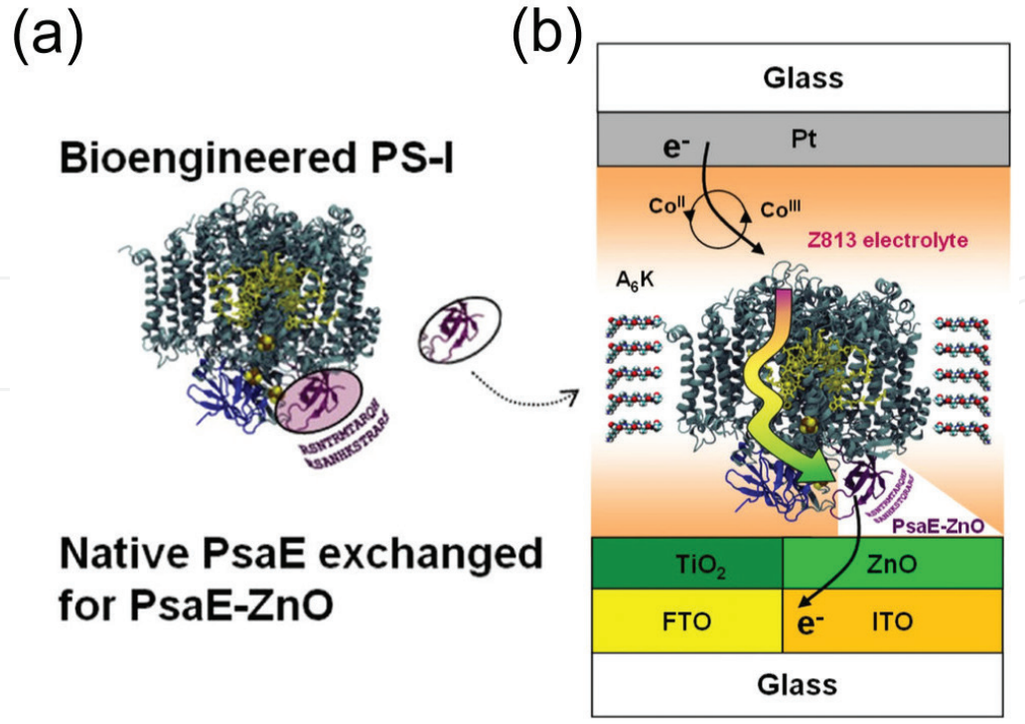

Figure 7. (a) Bioengineered modification of PS I by substitution of native PsaE with PsaE-ZnO. (b) Schematic electron transfer path in PS I-based biophotovoltaic cells. Adapted with permission of Ref. [35].

on a APTES grafted FTO substrate via electrostatic interaction between the anionic residues on the stromal side with cationic $-NH_3^+$ groups [14]. We adopted this approach and used APTES to functionalize the surface of TiO_2 thin film, TiO_2 nanotree array photoanodes and TiO_2-encapsulated plasmonic NPs in LHCII sensitized solar cells [25]. Clear improvement in protein attachment is indicated by the more intense and uniform greenish color on the APTES modified photoanode (**Figure 8a**).

Moreover, adsorption of the photosynthetic proteins onto internal surface of the mesoporous TiO_2 anode is also hindered by its much larger size (4–20 nm) than dye molecules (<1 nm), researchers strive to increase their loading capacity by engineering more open three-dimensional (3D) electrode architecture. The amount of the adsorbed proteins can be extracted into buffer solutions and quantitatively assessed from the absorption spectra of the extracted Chls in **Figure 8b** based on the following equation [37]:

$$\text{Chlsa}(a+b) = 17.6\ A^{646.6} + 7.34\ A^{663.6} \quad (1)$$

A is the absorbance at certain wavelength. By this means, the amount of LHCII trimers adsorbed on APTES-treated TiO_2 nanotrees was determined to be 2.5 folds of that on bare TiO_2 nanotrees. It can be derived from basic calculations that LHCII trimers containing 0.2 μg Chls are required to form a hexagonal close-packed monolayer on a flat 1 × 1 cm^2 surface. Since the adsorbed LHCII trimers were equivalent to 6.6 μg Chls, 33 times of that on the flat TiO_2 surface, it is evident that nanoscale LHCII trimers were able to penetrate into the 3D TiO_2 nanotree array and adsorb on a large surface area.

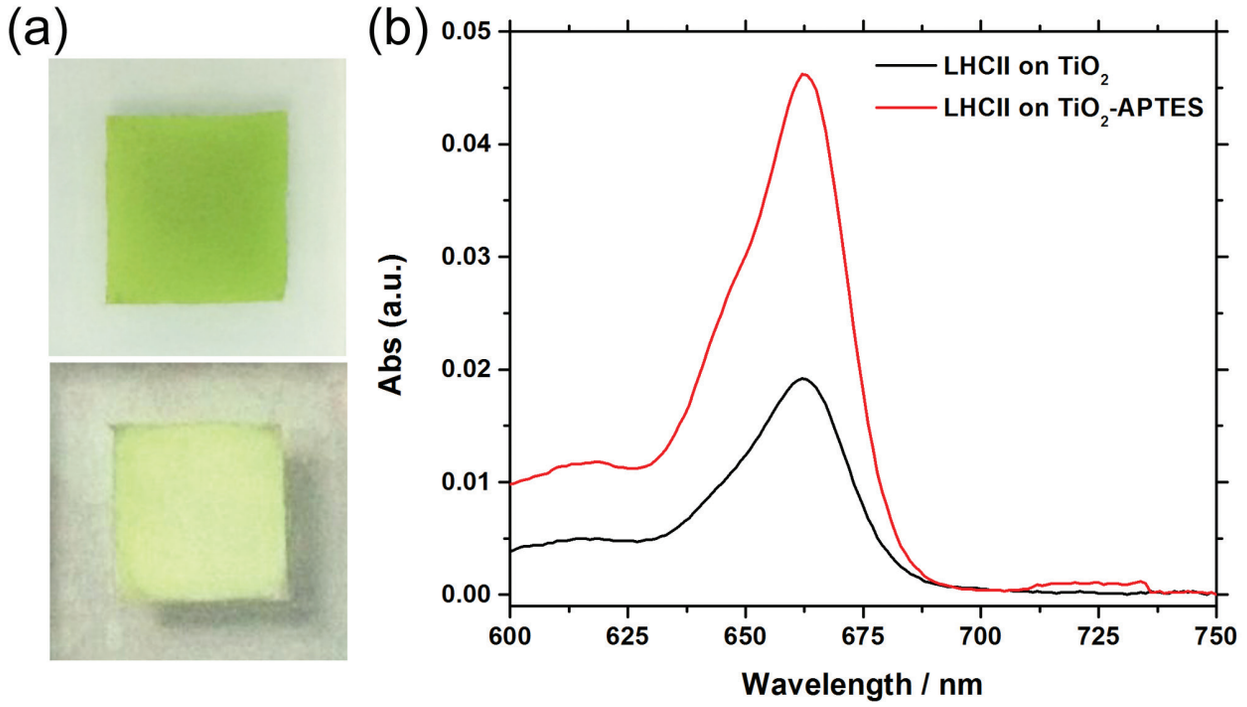

Figure 8. (a) The digital photographs of the LHCII-sensitized region of an APTES-treated TiO_2 nanotree array (top) and a bare TiO_2 nanotree array (bottom) (b) UV-Vis absorption of the chlorophylls pigment extracted from the LHCII trimers adsorbed on TiO_2 nanotree photoanodes with and without APTES functionalization. Reprinted with permission of Ref. [25].

3. Energy state coupling and charge transfer between photosynthetic proteins and TiO_2

3.1. General electron transfer in the biophotovoltaic cells with photosynthetic protein sensitized TiO_2 photoanodes

Similar to DSSCs, photocurrent generation by biophotovoltaic cells based on photosynthetic proteins sensitized TiO_2 photoanode is inextricably linked with the charge separation at the photosynthetic protein/TiO_2 interface. The energy state matching among photosynthetic proteins, semiconductive TiO_2, and redox mediators is crucial to enable the electron injection from photosynthetic proteins to TiO_2 as well as the electron refill from redox mediators to the proteins. The photoinduced electrons originate from Q band excitation of Chls. Since Chl is the major pigment contained in photosynthetic proteins, the energy levels of the photosynthetic proteins can be represented by the ground and excitation states of Chls Q band, and they can be determined by measuring the oxidation potential and the absorption spectrum of the photosynthetic proteins. **Figure 9** shows the electron transfer and energy level scheme of the biophotovoltaic cell based on LHCII aggregates as the sensitizer on thin film TiO_2 photoanode. Potentials are relative to the normal hydrogen electrode (NHE) [38]. Similar to DSSCs, when the chlorophylls in the photosynthetic proteins are photoexcited to the higher energy level Chl*, the electrons are able to inject into the less negative conduction band of TiO_2. In

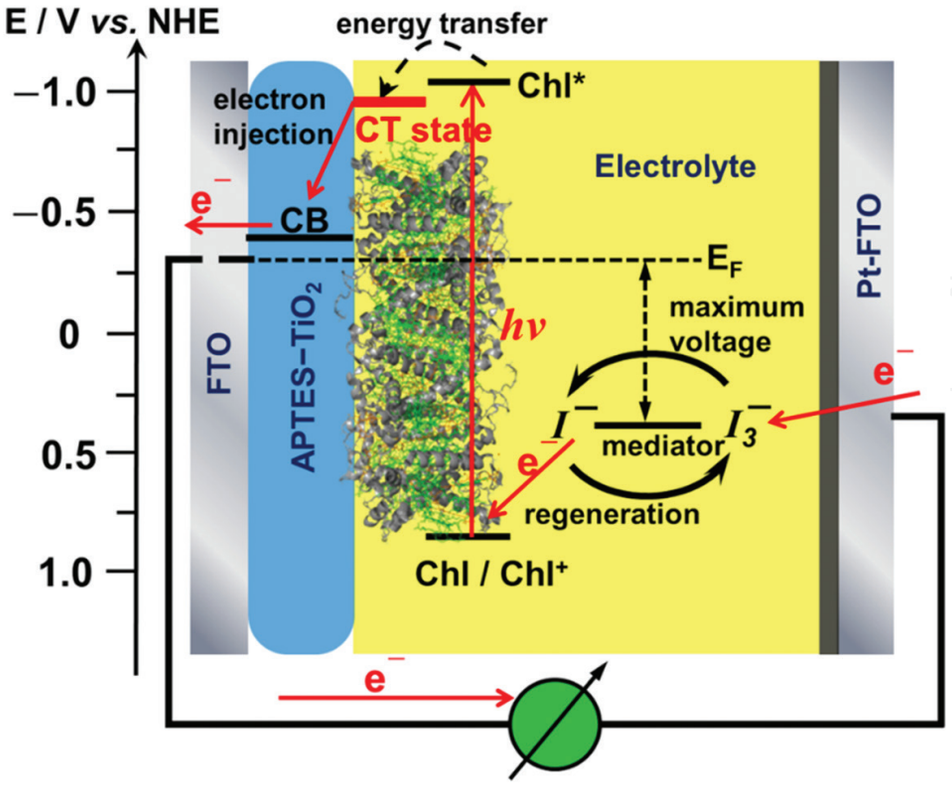

Figure 9. Electron transfer and energy level scheme of a photovoltaic device based on aggregated LHCII complexes. Reprinted with permission from Ref [38].

this step, the harvested solar energy is converted into anodic photocurrent. Meanwhile, the redox potential of the mediator should be more negative (i.e., in lower position in **Figure 9**) than the hole left at the ground state of Chlorophyll Ch^+ so that it can resupply an electron to the oxidized Chl, thus regenerating the sensitizer. The V_{OC} (maximum output voltage of solar cell) corresponds to the difference between the redox potential of the redox mediator and the Fermi level of the FTO current collector.

3.2. Effect of charge transfer state in LHCs

Comparing to artificial DSSCs, the biophotovoltaics involving photosynthesis complexes as sensitizers have two distinct features. First, the captured photon may go through a rapid internal energy transfer process to the charge-separation states. For example, **Figure 10A** shows that the excitation energy of LHCII at 496.5 nm is quickly transferred to the lower-energy Q band around 650–690 nm before giving fluorescence or producing charge separation. Second, the charge transfer process of densely assembled chlorophylls in photosynthetic protein complexes depends on the specific protein environments involving photosynthesis regulation through a photoprotective mechanism called non-photochemical quenching (NPQ) [9, 39–44]. Excess energy in the photo-excited chlorophylls was dissipated through specific LHCII protein aggregation [45]. The Chl excited states in the aggregated LHCII, unlike in isolated LHCII trimers, are severely quenched due to the formation of chlorophyll-chlorophyll coupled charge transfer (CT) states, which has been observed by the high-resolution hole-burning spectroscopy [46].

http://dx.doi.org/10.5772/intechopen.68744

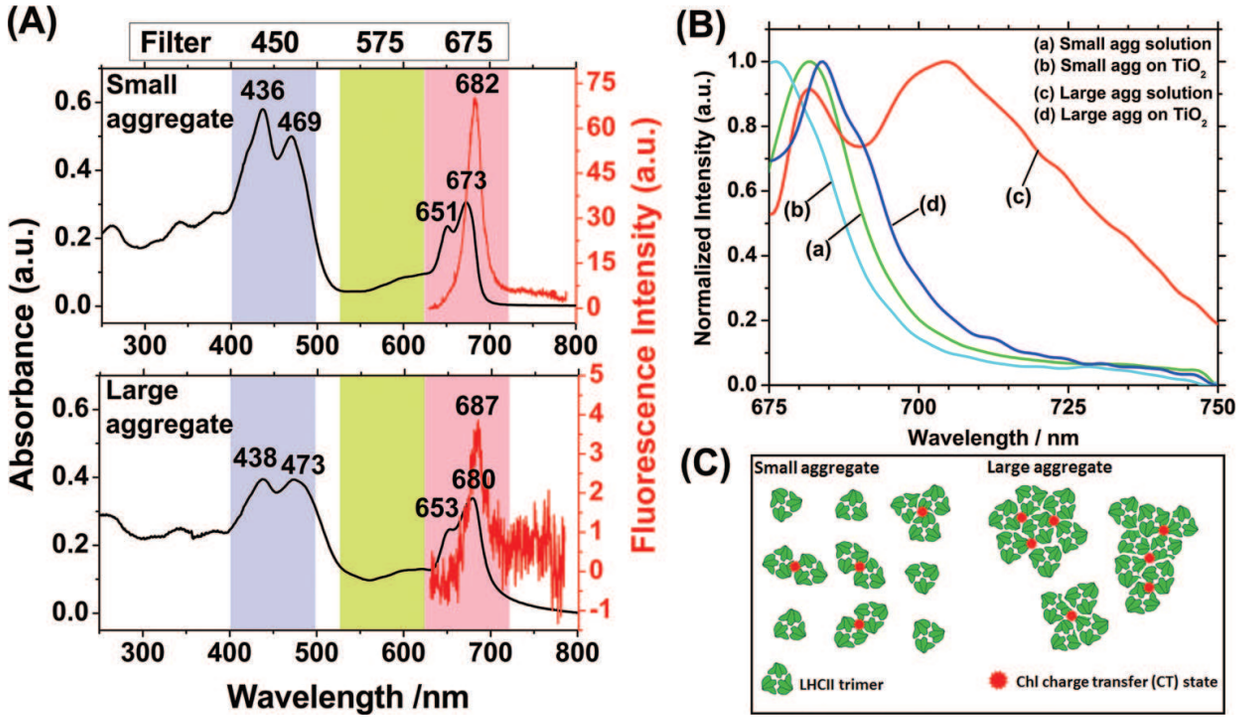

Figure 10. Absorption and emission properties of LHCII aggregates associated with the formation of CT states. (A) Absorption and fluorescence emission spectra (λ_{ex} = 496.5 nm) of small- and large-size LHCII aggregate in tricine buffer. (B) Normalized steady-state fluorescence emission spectra (λ_{ex} = 663 nm) of small- and large-size LHCII aggregate in solutions and deposited on the APTES-TiO_2-FTO photoanode surface, respectively. (C) Schematic illustration of the CT states (dots) formed in small and large aggregates. Reprinted with permission of Ref. [38].

Previous study revealed that the photovoltaic performance of the biophotovoltaic cell was correlated with strong coupling between the extensive CT states formed between the aggregated LHCIIs (schematically depicted in **Figure 10C**) and the TiO_2 conduction band. The CT states have slightly lower oxidation potential (i.e., less negative in energy level in **Figure 9**) than the excited state of chlorophylls due to their more reddish absorption and red tail in UV spectra (**Figure 10A**). The CT states couple with the TiO_2 conduction band more effectively, convinced by severe quench on the fluorescence emission of the CT states when the large LHCII aggregates were anchored on TiO_2 surface (as shown in **Figure 10B**). This strong coupling facilitated more efficient electron injection across LHCII/TiO_2 interface and resulted in larger photocurrent generation in the corresponding biophotovoltaic cells.

3.3. Effect of plasmonic nanoparticles

While the biophotovoltaic cells based on interfacing the artificial DSSC platform with the photosynthetic proteins provide useful insight into the fundamental photon capture and charge separation processes, their PCE is much lower than the conventional DSSCs using organic dye molecules (such as N719 [47]) as light harvesting antennas. Noble metal nanoparticles, that is, gold or silver nanoparticles, have been explored to enhance the solar cell performance utilizing their surface plasmonic resonance (SPR) effects that can enormously alter the optical absorption and emission of photosynthetic proteins near the nanoparticle surface [48]. An example of such solar cells is shown in **Figure 11** [25]. Enhancement of light absorption was observed for

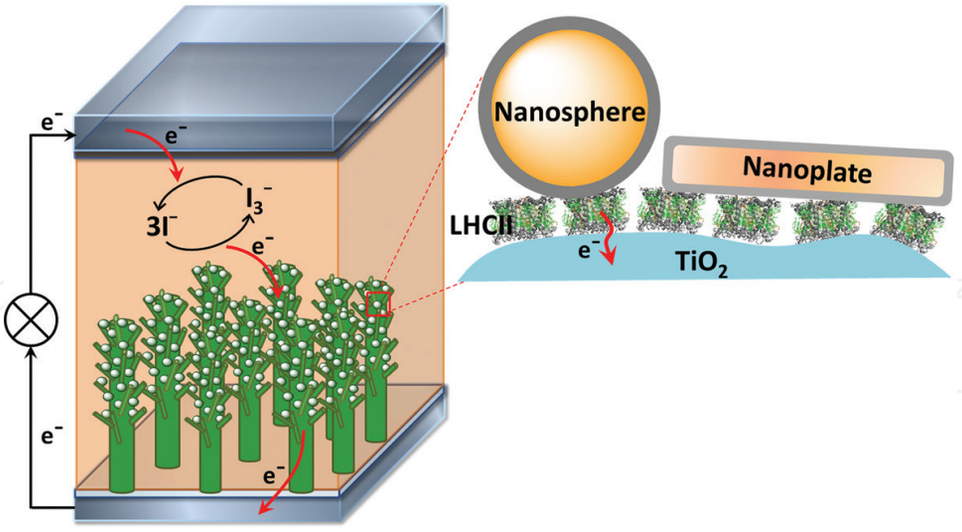

Figure 11. The structure of the plasmonic biophotovoltaic cell. The enlarged portion (in square) shows the binding of different PNPs on LHCII-sensitized TiO_2 nanotrees and the electron injection from LHCII to TiO_2 (curve arrow). Reprinted with permission of Ref. [25].

PSI attached to plasmonic nanoparticles (PNPs) [49]. The LHCs anchored on plasmonic gold or silver island substrates were able to generate 10- to 20-fold of fluorescence emission [50–52]. A theoretical model for SPR-enhanced free electron production and photocurrent generation was proposed based on PSI-RCs bound to Au and Ag nanocrystals [53]. The internal photosynthetic efficiency of PSI-RC was found to be strongly enhanced by the metal nanoparticles, which involved two competing effects, that is, plasmon enhanced light absorption of Chl molecules and energy transfer from Chl to metal nanoparticles [53]. These studies provide useful insights into energy-conversion devices involving the interplay between photosynthetic proteins and PNPs.

PNPs have already been widely employed in photovoltaic devices, including DSSCs [54–56] and emerging Perovskite solar cells [57, 58], to enhance the performance. However, the explanation of the interplays between PNPs and different light harvesting antennas is still ambiguous in each specific cases. Unlike single chromatic synthetic dye, photosynthetic proteins contain multiple pigments whose light harvesting and conversion involve intrinsic energy transfer among pigments and cofactors, inducing additional complexity to understand the plasmonic effects on the whole photovoltaic processes of the bio-hybrid systems. Recently, a bio-solar cell using natural extract graminoids coupled with silver nanoparticles (Ag-NPs) has been reported to achieve larger photocurrent [59]. First, incorporating plasmonic Ag-NPs (~13.8 nm in diameter) enables quenching the emission of the natural graminoid sensitizers and thus enhancing the electron collection efficiency. Meanwhile, the small size of the Ag-NPs barely takes up surface area for attachment of light-harvesting sensitizers. Second, a TiO_2(001) nanosheet structure provides a good surface for collection of solar-driven electrons from graminoids. Third, the ligand tethering enables good attachment between graminoids and Ag-NPs on the (100) face of TiO_2 nanosheet. The enhanced performance of the plasmonic biophotovoltaic cell in this case was attributed to the emission quenching by Ag-NPs for efficient collection of photoinduced electrons from graminoid complexes, as well as the efficient light trapping due to the plasmonic enhanced local electromagnetic field.

http://dx.doi.org/10.5772/intechopen.68744

We proposed another enhancement mechanism for plasmonic biophotovoltaics with the design shown in **Figure 12** [25]. Core-shell PNPs with a 2–5 nm TiO_2 shell and a plasmonic silver or gold core were hybridized with LHCII and incorporated into the aforementioned 3D TiO_2 nanotree photoanode for the plasmonic enhanced biophotovoltaic cells. Compared with the bare Ag NPs used in the above-discussed work [59], this core-shell structure has multiple functions. First, the hydrophilic nature of TiO_2 shell makes the PNP surface compatible for protein attachment [60]. Second, the semiconductive TiO_2 shell serves as an energy barrier to prevent electron recombination on the metallic core due to unwanted electron flow from the attached proteins to the metallic core [61]. Third, the TiO_2 shell acts as a protective armor to ensure the stability of the metallic core in the corrosive iodide electrolytes in solar cells [62]. These PNPs with different plasmonic resonance bands were able to enhance and manipulate the photon capture of LHCII at specific wavelength ranges. The photocurrent

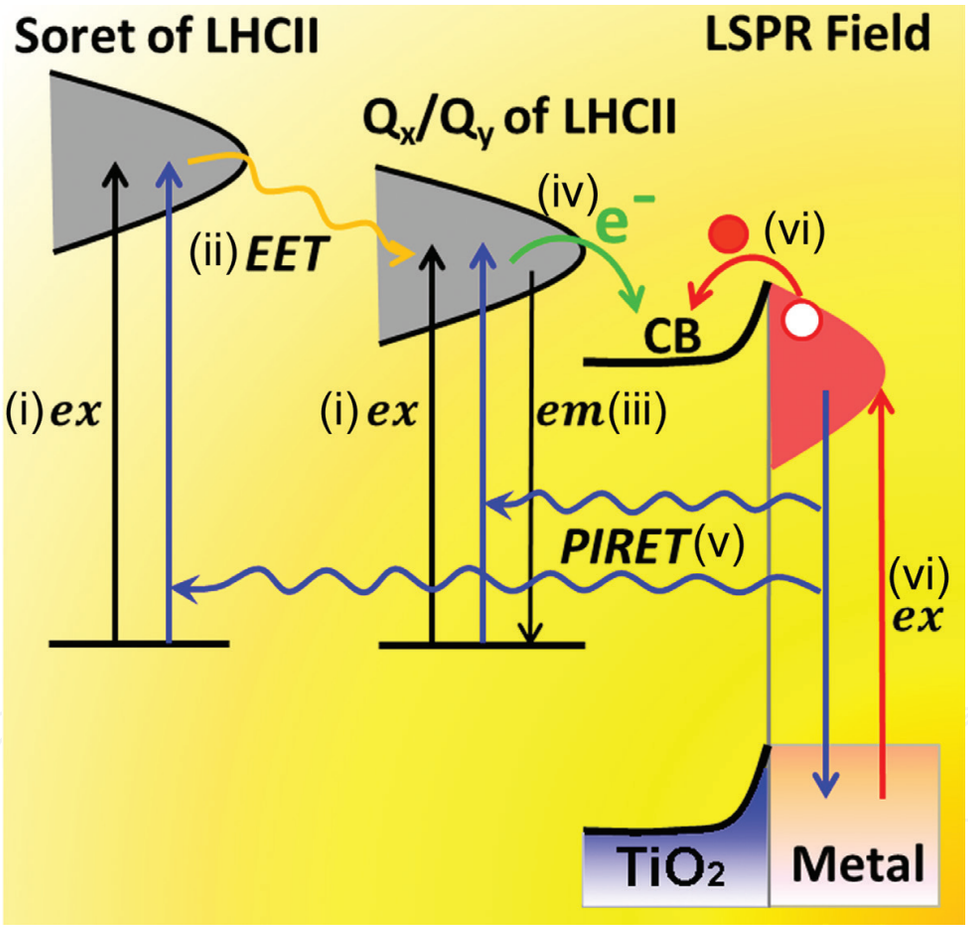

Figure 12. Schematic diagram of the energy and electron pathways in LHCII-PNP hybrid system. The LHCII trimers are excited by strong absorption of Chls' Soret and Q bands (i). The excited Chls go through an ultrafast excitation energy transfer (EET) from Soret band to Q band (ii) and then give fluorescence emission (iii) to return to the ground level. With LHCII attached to TiO_2 surface, a charge transfer process occurs, leading to injection of excited electrons in Q band to the conduction band (CB) of TiO_2 (iv). Thus, the fluorescence intensity is reduced. In the presence of the metallic core, further excitation to LHCII may occur due to plasmon-induced resonance energy transfer (PIRET) from PNPs to LHCII (v), resulting in larger electron injection from LHCII to TiO_2. At the meantime, the injection of hot electrons from the metal core of PNPs across the Schottky barrier (vi) leads to higher charge carrier density in TiO_2. Reprinted with permission from Ref. [25].

and incident photon-to-current efficiency (IPCE) of the plasmonic biophotovoltaic cell were achieved, while the fluorescence emission of excited LHCII was quenched along with shortened lifetime. Obviously, the electrons in the excited LHCII state flow efficiently through the TiO_2 network.

Cushing et al. [63, 64] elaborated that three mechanisms are involved charge generation in a semiconductor incorporated with plasmonic metal NPs, including light trapping based on scattering, hot electron/hole transfer, and plasmon-induced resonance energy transfer (PIRET) based on near-field. These are also applicable to the LHCII-PNP hybrids, with the possible mechanisms illustrated in **Figure 12**. During the excitation process, electrons are pumped from the ground state to the excited states of Soret band or Q band of LHCII. However, the excited Soret band quickly goes through an ultrafast excitation energy transfer (EET) to the Q band, as verified by a theoretical modeling [65]. Thus, all fluorescence emission from LHCIIs is at 683 nm, corresponding to a radiative relaxation for the excited electrons to return to the ground state of Q band. When LHCII is adsorbed on the TiO_2 surface, upon excitation a charge transfer process occurs, that is, the excited electrons in Q band are injected to the conduction band (CB) of TiO_2, resulting in the reduced fluorescence intensity. In the presence of the metallic core, the incident photons by plasmonic absorption generate a strong near-field oscillation with ~10 nm decay length, which can affect all LHCII adsorbed on the surface of the ~2–3-nm-thick TiO_2 shell. A strong PIRET is enabled by the strong dipole-dipole coupling between the plasmon and LHCII, leading to enhanced LHCII excitations at Soret and Q bands. More efficient electron injection from LHCII to TiO_2 is also facilitated by the near-field and thus quenches the fluorescence emission though PIRET induces higher LHCII excitation. These effects collectively enhance the photocurrent of the corresponding plasmonic biophotovoltaic cells. In addition, the plasmonic hot electrons excited at the metal core of PNPs may overcome the Schottky barrier at the metal-TiO_2 interface, raise the charge carrier density in TiO_2 shell, and therefore the charge collection efficiency. Details about such interfacial activity are unravelled in the next section.

4. Hot electron injection from plasmonic metal to TiO_2

Schottky barrier is an energy barrier for electrons formed at the junction of metal and semiconductor where their fermi levels merge together to achieve thermal equilibrium, leading to the band bending and blocking the electron flow across the junction. The energy band diagram of Schottky contact is illustrated in **Figure 13**. The height of Schottky barrier equals to the subtraction of work function of metal with the bandgap of semiconductor, and it is usually much smaller in value (e.g., ~0.9 eV for Au/TiO_2 [66] and ~0.2 eV for Ag/TiO_2 [67]) than the semiconductor bandgap (i.e., 3.2 eV for anatase TiO_2). Recent studies proposed hot electrons from plasmonic-excited metal cores could easily overcome this energy barrier and be injected into the TiO_2 conduction band, resulting in a new mechanism for plasmon enhancement to DSSCs [68]. In general, the injected hot electrons are considered to be either being converted into photocurrent or functioning as charge carriers in the semiconductor matrix [69]. The photocurrent generated by direct hot electron transfer across the Schottky barrier has been

http://dx.doi.org/10.5772/intechopen.68744

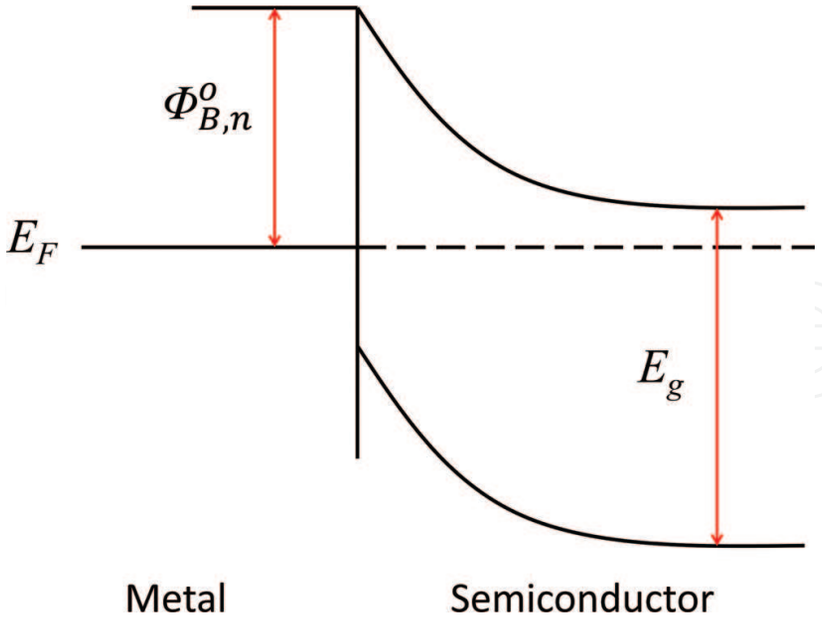

Figure 13. Energy band diagram of Schottky barrier formed at metal/n-type semiconductor interface.

collected and utilized for photodetection and photovoltaics based on well-designed devices with a complete circuit allowing refilling electrons back to the metal [70–73]. However, for the metal@TiO_2 NPs embedded in the mesoporous TiO_2 film in DSSCs, the sustainability of the photocurrent generation from hot electron injection is under debate considering that the metal core is unaccessible to the electron donors or the external circuit, which is needed for charge regeneration. On the other hand, the initially injected hot electrons may be converted into steady-state charge carriers and sufficiently raise the conductivity of the mesoporous TiO_2 frame, as has been indirectly demonstrated by enhanced photoconductivity in metal coupled semiconductors [74, 75]. In addition, a recent study by Cushing et al. reported that metal@TiO_2 and metal@SiO_2@TiO_2 NPs can also enhance DSSCs by exciting surrounding TiO_2 matrix and dye molecules with near-field-based plasmon-induced resonance energy transfer (PIRET) beside hot electron injection [63]. In the previous section, we have also discussed such effects on the plasmonic biophotovoltaic cells based on hybrids of natural LHCII and PNP [25]. Actually, these three effects are mixed in most plasmonic photovoltaic cells.

In order to sort out the contributions of hot electron injection, we propose a strategy by comparing the photoconductivity and the photovoltaic properties of the same material, that is, Au@TiO_2 network in two model devices, that is, a micro-gap electrode and a DSSC [76]. The core-shell structure consisting of isolated Au NPs embedded at the nodes of a nanostructured TiO_2 network was used as the bridging material in the micro-gap between two Au electrodes and as the mesoporous film on a DSSC anode to measure photoconductance and photocurrent, respectively. Enhancements on the photoconductance and the photocurrent were observed on both devices, with distinct dependence on the illumination wavelength (**Figure 14A** and **B**). This difference was explained with the scheme drawn in **Figure 14C** and **D**. The enhanced photoconductance is ascribed to the hot electron injection from Au NPs to TiO_2 that increase the charge carrier density of the TiO_2 network. This interfacial electron injection across the Au/TiO_2

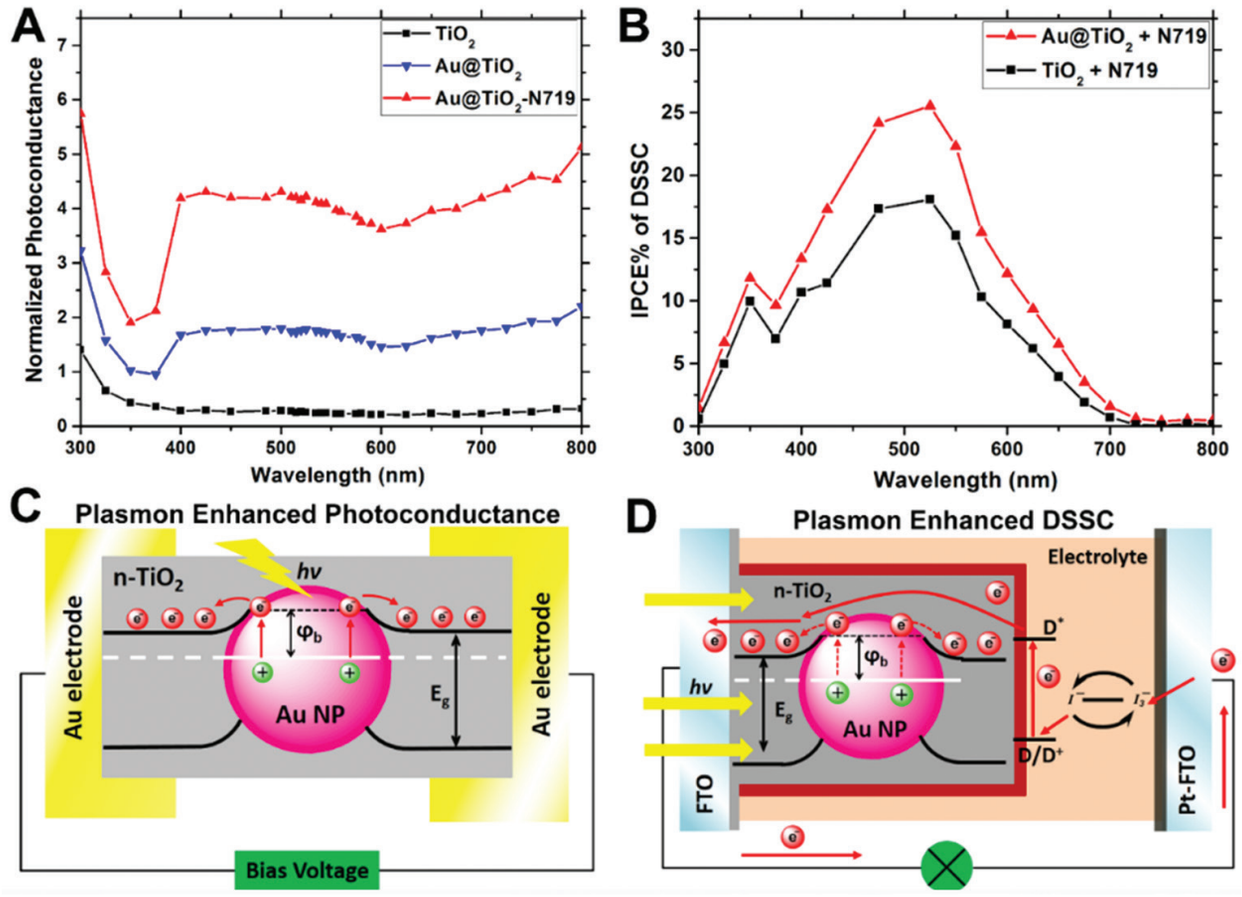

Figure 14. (A and B) Wavelength dependence of photoconductance and incident photon-to-current efficiency (IPCE) studies and (C and D) the schematics of the possible enhancement mechanisms for the Au@TiO_2 network on the micro-gap electrode and in the DSSC, respectively. Reprinted with permission from Ref. [76].

Schottky barrier (~0.9 eV) can be easily realized under illumination over the whole visible range, allowing extending the enhancement effect to the light in the near-infrared region. The photon energies in wavelength larger than 700 nm are smaller than the energy of semiconductor band gap, Au plasmonic band, and dye absorption band. In the DSSC, the plasmonic generated hot electrons cannot be the source of continuous steady-state photocurrent, since the Au NPs embedded within the TiO_2 shell are not accessible by the regenerating agents. The major contribution for the photocurrent enhancement must be the surface plasmonic resonance effect that can only be induced by the illumination in the range where the plasmonic band of Au NPs is resonant with dye absorption band (i.e., band overlap in absorption spectra). However, the injected hot electrons are sufficient to raise the charge carrier density in TiO_2 and reduce the series resistance and charge transfer resistance in the corresponding DSSCs. This facilitates the transport of the photo-induced electrons through the TiO_2 network.

5. Conclusions

This chapter reviews the synergistic interplay among TiO_2 photoanode, biophotosensitizers (e.g., LHCII) and plasmonic nanoparticles in the photovoltaic devices. The effectiveness of

TiO_2 as an interfacial photoanode material compatible with photosynthetic proteins and plasmonic nanoparticles was demonstrated. The electron injection from excited LHCII to TiO_2 conduction band was realized due to the perfect match of energy bands, resulting in the photocurrent generation in the LHCII sensitized TiO_2 solar cells. The charge separation at LHCII/TiO_2 interface can be facilitated by incorporation of PNPs. This effect can be ascribed to the near-field-assisted PIRET from PNPs to LHCII across the TiO_2 interfacial layer. The hot electron injection across Schottky barrier from plasmonic core into TiO_2 network can increase the charge carrier density in TiO_2, leading to the increase of photoconductivity and the improved photovoltaic performance of TiO_2-based photoanode. Understanding of these fundamental energy/charge transfer processes and interface properties will inspire future optoelectronic devices with smart designs for outstanding performance.

Acknowledgements

This work was supported by the National Science Foundation (NSF) EPSCoR Award EPS-0903806, a National Aeronautics and Space Administration (NASA) grant NNX13AD42 A, and the matching funds to these two grants provided by the State of Kansas.

Author details

Yiqun Yang[1] and Jun Li[2]*

*Address all correspondence to: junli@ksu.edu

1 Xavier University of Louisiana, New Orleans, LA, United States

2 Kansas State University, Manhattan, KS, United States

References

[1] Chen X, Mao SS. Titanium dioxide nanomaterials: synthesis, properties, modifications, and applications. Chemical Reviews. 2007;**107**:2891-2959

[2] O' Regan B, Grätzel M. A low-cost, high-efficiency solar-cell based on dye-sensitized colloidal TiO_2 films. Nature. 1991;**353**:737-740. DOI: 10.1038/353737a0

[3] Miki N. Liquid encapsulation technology for microelectromechanical systems. In: Kenichi Takahata editor, Advances in Micro/Nano Electromechanical Systems and Fabrication Technologies, In Tech, Croatia-European Union; 2013. DOI: 10.5772/55514

[4] Yella A, Lee H-W, Tsao HN, Yi C, Chandiran AK, Nazeeruddin MK, Diau E, W-G, Yeh C-Y, Zakeeruddin SM, Grätzel M. Porphyrin-sensitized solar cells with cobalt (II/III)–based Redox electrolyte exceed 12 percent efficiency. Science. 2011;**334**:629-634. DOI: 10.1126/science.1209688

[5] Burschka J, Pellet N, Moon S-J, Humphry-Baker R, Gao P, Nazeeruddin M. K Gratzel M. Sequential deposition as a route to high-performance perovskite-sensitized solar cells. Nature. 2013;**499**:316-319. DOI: 10.1038/nature12340

[6] Giordano F, Abate A, Correa Baena JP, Saliba M, Matsui T, Im SH, Zakeeruddin SM, Nazeeruddin MK, Hagfeldt A, Graetzel M. Enhanced electronic properties in mesoporous TiO_2 via lithium doping for high-efficiency perovskite solar cells. Nature Communications. 2016;**7**:10379. DOI: 10.1038/ncomms10379

[7] Various Authors, Photosystem, Wikipedia [Internet]. 2015. Available from: https://commons.wikimedia.org/wiki/File%3AThylakoid_membrane_3.svg

[8] Fleming GR, Schlau-Cohen GS, Amarnath K, Zaks J. Design principles of photosynthetic light-harvesting. Faraday Discussions. 2012;**155**:27-41. DOI: 10.1039/C1FD00078K

[9] Caffarri S, Kouřil R, Kereïche S, Boekema EJ, Croce R. Functional architecture of higher plant photosystem II supercomplexes. EMBO J. 2009;**28**:3052-3063. DOI: 10.1038/emboj.2009.232

[10] Liu Z, Yan H, Wang K, Kuang T, Zhang J, Gui L, An X, Chang W. Crystal structure of spinach major light-harvesting complex at 2.72 Å resolution. Nature. 2004;**428**:287-292. DOI: 10.1038/nature02373

[11] Ondersma JW, Hamann TW. Recombination and redox couples in dye-sensitized solar cells. Coordination Chemistry Reviews 2013;**257**:1533-1543. DOI: 10.1016/j.ccr.2012.09.010

[12] Ludin NA, Al-Alwani Mahmoud AM, Bakar Mohamad A, Kadhum AAH, Sopian K, Abdul Karim NS. Review on the development of natural dye photosensitizer for dye-sensitized solar cells. Renewable & Sustainable Energy Reviews. 2014;**31**:386-396. DOI: 10.1016/j.rser.2013.12.001

[13] Hug H, Bader M, Mair P, Glatzel T. Biophotovoltaics: Natural pigments in dye-sensitized solar cells. Applied Energy. 2014;**115**:216-225. DOI: 10.1016/j.apenergy.2013.10.055

[14] Nagata M, Amano M, Joke T, Fujii K, Okuda A, Kondo M, Ishigure S, Dewa T, Iida K, Secundo F, Amao Y, Hashimoto H, Nango M. Immobilization and photocurrent activity of a light-harvesting antenna complex II, LHCII, isolated from a plant on electrodes. ACS Macro Letters. 2012;**1**:296-299. DOI: 10.1021/mz200163e

[15] Narayan MR. Review: Dye sensitized solar cells based on natural photosensitizers. Renewable & Sustainable Energy Reviews. 2012;**16**:208-215. DOI: 10.1016/j.rser.2011.07.148

[16] Yu D; Zhu G, Liu S, Ge B, Huang F. Photocurrent activity of light-harvesting complex II isolated from spinach and its pigments in dye-sensitized TiO_2 solar cell. International Journal of Hydrogen Energy. 2013;**38**:16740-16748. DOI: 10.1016/j.ijhydene.2013.02.114

[17] Yu D, Wang M, Zhu G, Ge B, Liu S, Huang F. Enhanced photocurrent production by bio-dyes of photosynthetic macromolecules on designed TiO_2 film. Scientific Reports. 2015;**5**:9375. DOI: 10.1038/srep09375

[18] Wang M, Bai J, Le Formal F, Moon S-J, Cevey-Ha L, Humphry-Baker R, Grätzel C, Zakeeruddin SM, Grätzel M. Solid-State dye-eensitized solar cells using ordered TiO_2 nanorods on transparent conductive oxide as photoanodes. The Journal of Physical Chemistry C. 2012;**116**:3266-3273. DOI: 10.1021/jp209130x

[19] Tétreault N, Horváth E, Moehl T, Brillet J, Smajda R, Bungener S, Cai N, Wang P, Zakeeruddin SM, Forró L, Magrez A, Grätzel M. High-efficiency solid-state dye-sensitized solar cells: fast charge extraction through self-assembled 3D fibrous network of crystalline TiO_2 nanowires. ACS Nano. 2010;**4**:7644-7650. DOI: 10.1021/nn1024434

[20] Yu H, Zhang S, Zhao H, Xue B, Liu P, Will G. High-performance TiO_2 photoanode with an efficient electron transport network for dye-sensitized solar cells. The Journal of Physical Chemistry C. 2009;**113**:16277-16282. DOI: 10.1021/jp9041974

[21] Sheng X, He D, Yang J, Zhu K, Feng X. Oriented assembled TiO_2 hierarchical nanowire arrays with fast electron transport properties. Nano letters. 2014;**14**:1848-1852. DOI: 10.1021/nl4046262

[22] Tetreault N, Gratzel M. Novel nanostructures for next generation dye-sensitized solar cells. Energy and Environmental Science. 2012;**5**:8506-8516. DOI: 10.1039/C2EE03242B

[23] Shankar K, Mor GK, Prakasam HE, Yoriya S, Paulose M, Varghese OK, Grimes CA. Highly-ordered TiO_2 nanotube arrays up to 220 μm in length: Use in water photoelectrolysis and dye-sensitized solar cells. Nanotechnology. 2007;**18**:065707

[24] Sauvage F, Di Fonzo F, Li Bassi A, Casari C. S, Russo V, Divitini G, Ducati C, Bottani CE, Comte P, Graetzel M. Hierarchical TiO_2 photoanode for dye-sensitized solar cells. Nano Letters. 2010;**10**:2562-2567. DOI: 10.1021/nl101198b

[25] Yang Y, Gobeze HB, D'Souza F, Jankowiak R, Li J. Plasmonic enhancement of biosolar cells employing light harvesting complex II incorporated with core–shell metal@ TiO_2 nanoparticles. Advanced Materials Interfaces. 2016;**3**:1600371. DOI: 10.1002/admi.201600371

[26] Wu W-Q, Lei B.-X, Rao H-S, Xu Y-F, Wang Y-F, Su C-Y, Kuang D-B. Hydrothermal fabrication of hierarchically Anatase TiO_2 nanowire arrays on FTO glass for dye-sensitized solar cells. Scientific Reports. 2013;**3**:1352. DOI: 10.1038/srep01352

[27] Yang Y. Integration of photosynthetic pigment-protein complexes in dye sensitized solar cells towards plasmonic-enhanced biophotovoltaics [Thesis]. Proquest: Kansas State University, **2016**

[28] Park NG, van de Lagemaat J, Frank AJ. Comparison of dye-sensitized rutile- and Anatase-based TiO_2 solar cells. The Journal of Physical Chemistry B. 2000;**104**:8989-8994. DOI: 10.1021/jp994365l

[29] Schattauer S, Reinhold B, Albrecht S, Fahrenson C, Schubert M, Janietz S, Neher D. Influence of sintering on the structural and electronic properties of TiO_2 nanoporous

layers prepared via a non–sol–gel approach. Colloid and Polymer Science 2012;**290**:1843-1854. DOI: 10.1007/s00396-012-2708-9

[30] Burke A, Ito S, Snaith H, Bach U, Kwiatkowski J, Grätzel M. The function of a TiO_2 compact layer in dye-sensitized solar cells incorporating "Planar" organic dyes. Nano Letters. 2008;**8**:977-981. DOI: 10.1021/nl071588b

[31] Hore S, Kern R. Implication of device functioning due to back reaction of electrons via the conducting glass substrate in dye sensitized solar cells. Applied Physics Letters. 2005;**87**:263504. DOI: 10.1063/1.2149215

[32] Zheng Y, Klankowski S, Yang Y, Li J. Preparation and characterization of TiO_2 barrier layers for dye-sensitized solar cells. ACS applied materials and interfaces. 2014;**6**:10679-10686. DOI: 10.1021/am502421w

[33] Brennan BJ, Llansola Portoles MJ, Liddell PA, Moore TA, Moore AL, Gust D. Comparison of silatrane, phosphonic acid, and carboxylic acid functional groups for attachment of porphyrin sensitizers to TiO_2 in photoelectrochemical cells. Physical Chemistry Chemical Physics: PCCP. 2013;**15**:16605-16614. DOI: 10.1039/C3CP52156G

[34] Zhang L, Cole JM. Anchoring groups for dye-sensitized solar cells. ACS Applied Materials and Interfaces. 2015;**7**:3427-3455. DOI: 10.1021/am507334m

[35] Mershin A, Matsumoto K, Kaiser L, Yu D, Vaughn M, Nazeeruddin MK, Bruce BD, Graetzel M, Zhang S. Self-assembled photosystem-I biophotovoltaics on nanostructured TiO_2 and ZnO. Scientific Reports. 2012;**2**:234. DOI: 10.1038/srep00234

[36] Gordiichuk PI, Wetzelaer G-J, AH, Rimmerman D, Gruszka A, de Vries JW, Saller M, Gautier DA, Catarci S, Pesce D, Richter S, Blom PWM, Herrmann A. Solid-state biophotovoltaic cells containing photosystem I. Advanced Materials. 2014;**26**:4863-4869. DOI: 10.1002/adma.201401135

[37] Porra RJ, Thompson WA, Kriedemann PE. Determination of accurate extinction coefficients and simultaneous equations for assaying chlorophylls a and b extracted with four different solvents: verification of the concentration of chlorophyll standards by atomic absorption spectroscopy. Biochimica et Biophysica Acta (BBA)—Bioenergetics. 1989;**975**:384-394. DOI: 10.1016/S0005-2728(89)80347-0

[38] Yang Y, Jankowiak R, Lin C, Pawlak K, Reus M, Holzwarth AR, Li J. Effect of the LHCII pigment-protein complex aggregation on photovoltaic properties of sensitized TiO_2 solar cells. Physical Chemistry Chemical Physics. 2014;**16**:20856-20865. DOI: 10.1039/C4CP03112A

[39] Johnson M. P, Goral TK, Duffy CDP, Brain APR, Mullineaux CW, Ruban AV. Photoprotective energy dissipation involves the reorganization of photosystem II light-harvesting complexes in the grana membranes of spinach chloroplasts. Plant Cell. 2011;**23**:1468-1479. DOI: 10.1105/tpc.110.081646

[40] Holzwarth AR, Miloslavina Y, Nilkens M, Jahns P. Identification of two quenching sites active in the regulation of photosynthetic light-harvesting studied by time-resolved fluorescence. Chemical Physics Letters. 2009;**483**:262-267. DOI: 10.1016/j.cplett.2009.10.085

[41] Belgio E, Duffy CDP, Ruban AV. Switching light harvesting complex II into photoprotective state involves the lumen-facing apoprotein loop. Physical Chemistry Chemical Physics: PCCP. 2013;**15**:12253-12261. DOI: 10.1039/c3cp51925b

[42] Ruban AV, Berera R, Ilioaia C, van Stokkum IHM, Kennis JTM, Pascal AA, van Ameron gen H, Robert B, Horton P, van Grondelle R. Identification of a mechanism of photoprotective energy dissipation in higher plants. Nature. 2007;**450**:575-578. DOI: 10.1038/nature06262

[43] Holzwarth AR, Jahns P: NPQ mechanisms in intact organisms as derived from ultrafast fluorescence kinetics studies. In: Govindjee, Sharkey, Thomas D, editors. Advances in Photosynthesis and Respiration, Springer Science, Berlin, Germany; **2014**. pp. 129-156

[44] Miloslavina Y, Wehner A, Lambrev PH, Wientjes E, Reus M, Garab G, Croce R, Holzwarth AR. Far-red fluorescence: A direct spectroscopic marker for LHCII oligomer formation in non-photochemical quenching. FEBS Letters. 2008;**582**:3625-3631. DOI: 10.1016/j.febslet.2008.09.044

[45] Magdaong N, Enriquez M, LaFountain A, Rafka L, Frank H. Effect of protein aggregation on the spectroscopic properties and excited state kinetics of the LHCII pigment-protein complex from green plants. Photosynthesis Research. 2013;**118**:18. DOI: 10.1007/s11120-013-9924-0

[46] Kell A, Feng X, Lin C, Yang Y, Li J Reus M, Holzwarth AR, Jankowiak R. Charge-transfer character of the low-energy Chl a Qy absorption band in aggregated light harvesting complexes II. The Journal of Physical Chemistry B. 2014;**118**:6086-6091. DOI: 10.1021/jp501735p

[47] Gratzel M. Recent advances in sensitized mesoscopic solar cells. Accounts of Chemical Research. 2009;**42**:1788-1798. DOI: 10.1021/ar900141y

[48] Mackowski S. Hybrid nanostructures for efficient light harvesting. Journal of Physics: Condensed Matter. 2010;**22**:193102. DOI: 10.1088/0953-8984/22/19/193102

[49] Carmeli I, Lieberman I, Kraversky L, Fan Z, Govorov AO, Markovich G, Richter S. Broad band enhancement of light absorption in photosystem I by metal nanoparticle antennas. Nano Letters. 2010;**10**:2069-2074. DOI: 10.1021/nl100254j

[50] Czechowski N, Nyga P, Schmidt M, Brotosudarmo TP, Scheer H, Piatkowski D, Mackowski S. Absorption enhancement in peridinin-chlorophyll-protein light-harvesting complexes coupled to semicontinuous silver film. Plasmonics. 2012;**7**:115-121. DOI: 10.1007/s11468-011-9283-7

[51] Mackowski S, Wörmke S, Maier AJ, Brotosudarmo THP, Harutyunyan H, Hartschuh A, Govorov A. O, Scheer H, Bräuchle C. Metal-enhanced fluorescence of chlorophylls in light-harvesting complexes. Nano Letters. 2008;**8**:558-564. DOI: 10.1021/nl072854o

[52] Beyer SR, Ullrich S, Kudera S, Gardiner AT, Cogdell R. J, Köhler J. Hybrid nanostructures for enhanced light-harvesting: Plasmon Induced Increase in Fluorescence from Individual Photosynthetic Pigment-Protein Complexes. Nano Letters. 2011;**11**:4897-4901. DOI: 10.1021/nl202772h

[53] Govorov AO, Carmeli I. Hybrid structures composed of photosynthetic system and metal nanoparticles: Plasmon Enhancement Effect. Nano Letters. 2007;**7**:620-625. DOI: 10.1021/nl062528t

[54] Atwater HA, Polman A. Plasmonics for improved photovoltaic devices. Nature Materials. 2010;**9**:205-213. DOI: 10.1038/nmat2629

[55] Dang X, Qi J, Klug MT, Chen P-Y, Yun DS, Fang NX, Hammond PT, Belcher AM. Tunable localized surface plasmon-enabled broadband light-harvesting enhancement for high-efficiency panchromatic dye-sensitized solar cells. Nano Letters. 2013;**13**:637-642. DOI: 10.1021/nl3043823

[56] Ding B, Lee BJ, Yang MJ, Jung HS, Lee JK. Surface-plasmon assisted energy conversion in dye-sensitized solar cells. Advanced Energy Materials. 2011;**1**:415-421. DOI: 10.1002/aenm.201000080

[57] Zhang W, Saliba M, Stranks SD, Sun Y, Shi X, Wiesner U, Snaith HJ. Enhancement of perovskite-based solar cells employing core–shell metal nanoparticles. Nano Letters. 2013;**13**:4505-4510. DOI: 10.1021/nl4024287

[58] Saliba M, Zhang W, Burlakov VM, Stranks SD, Sun Y, Ball JM, Johnston MB, Goriely A, Wiesner U, Snaith HJ. Plasmonic-induced photon recycling in metal halide perovskite solar cells. Advanced Functional Materials. 2015;**25**:5038-5046. DOI: 10.1002/adfm.201500669

[59] Adhyaksa GWP, Prima EC, Lee DK, Ock I, Yatman S, Yuliarto B, Kang JK. A light harvesting antenna using natural extract graminoids coupled with plasmonic metal nanoparticles for bio-photovoltaic cells. Advanced Energy Materials. 2014;**4**:1400470-1400477. DOI: 10.1002/aenm.201400470

[60] Wang Y, Wen C, Hodgson P, Li Y. Biocompatibility of TiO_2 nanotubes with different topographies. Journal of Biomedical Materials Research Part A. 2014;**102**:743-751. DOI: 10.1002/jbm.a.34738

[61] Du J, Qi J, Wang D, Tang Z. Facile synthesis of Au@TiO_2 core-shell hollow spheres for dye-sensitized solar cells with remarkably improved efficiency. Energy & Environmental Science. 2012;**5**:6914-6918. DOI: 10.1039/C2EE21264A

[62] Liu W-L, Lin F-C, Yang Y-C, Huang C-H, Gwo S, Huang MH, Huang J-S. The influence of shell thickness of Au@TiO_2 core-shell nanoparticles on the plasmonic enhancement effect in dye-sensitized solar cells. Nanoscale. 2013;**5**:7953-7962. DOI: 10.1039/C3NR02800C

[63] Cushing SK, Li J, Bright J, Yost BT, Zheng P, Bristow AD, Wu N. Controlling plasmon-induced resonance energy transfer and hot electron injection processes in metal@TiO_2 core–shell nanoparticles. The Journal of Physical Chemistry C. 2015;**119**:16239-16244. DOI: 10.1021/acs.jpcc.5b03955

[64] Cushing SK, Wu N. Progress and perspectives of plasmon-enhanced solar energy conversion. The Journal of Physical Chemistry Letters. 2016;**7**:666-675. DOI: 10.1021/acs.jpclett.5b02393

[65] Götze JP, Kröner D, Banerjee S, Karasulu B, Thiel W. Carotenoids as a shortcut for chlorophyll soret-to-Q band energy flow. ChemPhysChem. 2014;**15**:3392-3401. DOI: 10.1002/cphc.201402233

[66] Lee YK, Park J, Park JY. The effect of dye molecules and surface plasmons in photon-induced hot electron flows detected on Au/TiO_2 Nanodiodes. Journal of Physical Chemistry C. 2012;**116**:18591-18596. DOI: 10.1021/jp303099w

[67] Jiang Z, Zhu J, Liu D, Wei W, Xie J, Chen M. In situ synthesis of bimetallic Ag/Pt loaded single-crystalline anatase TiO_2 hollow nano-hemispheres and their improved photocatalytic properties. CrystEngComm. 2014;**16**:2384-2394. DOI: 10.1039/C3CE41949E

[68] Jang YH, Jang YJ, Kochuveedu ST, Byun M, Lin Z, Kim DH. Plasmonic dye-sensitized solar cells incorporated with Au-TiO_2 nanostructures with tailored configurations. Nanoscale. 2014;**6**:1823-1832. DOI: 10.1039/C3NR05012B

[69] Clavero C. Plasmon-induced hot-electron generation at nanoparticle/metal-oxide interfaces for photovoltaic and photocatalytic devices. Nature Photonics. 2014;**8**:95-103. DOI: 10.1038/nphoton.2013.238

[70] Knight MW, Sobhani H, Nordlander P, Halas NJ. Photodetection with active optical antennas. Science. 2011;**332**:702-704. DOI: 10.1126/science.1203056

[71] McFarland EW, Tang J. A photovoltaic device structure based on internal electron emission. Nature. 2003;**421**:616-618

[72] Tian Y, Tatsuma T. Mechanisms and applications of plasmon-induced charge separation at TiO_2 films loaded with gold nanoparticles. Journal of the American Chemical Society. 2005;**127**:7632-7637. DOI: 10.1021/ja042192u

[73] Chen ZH, Tang YB, Liu CP, Leung YH, Yuan GD, Chen LM, Wang YQ, Bello I, Zapien JA, Zhang WJ, Lee CS, Lee ST. Vertically aligned ZnO nanorod arrays sentisized with gold nanoparticles for Schottky barrier photovoltaic cells. The Journal of Physical Chemistry C. 2009;**113**:13433-13437. DOI: 10.1021/jp903153w

[74] Son M-S, Im J-E, Wang K-K, Oh S-L, Kim Y-R, Yoo K-H. Surface plasmon enhanced photoconductance and single electron effects in mesoporous titania nanofibers loaded with gold nanoparticles. Applied Physics Letters. 2010;**96**:023115. DOI: 10.1063/1.3291052

[75] Mubeen S, Hernandez-Sosa G, Moses D, Lee J, Moskovits M. Plasmonic photosensitization of a wide band gap semiconductor: Converting plasmons to charge carriers. Nano Letters. 2011;**11**:5548-5552. DOI: 10.1021/nl203457v

[76] Yang Y, Wu J, Li J. Correlation of the plasmon-enhanced photoconductance and photovoltaic properties of core-shell Au@ TiO_2 network. Applied Physics Letters. 2016;**109**:091604